Superconducting bearings

2000 Supercond. Sci. Technol. 13 R1

(http://iopscience.iop.org/0953-2048/13/2/201)

Supercond. Sci. Technol. **13** (2000) R1–R15. Printed in the UK PII: S0953-2048(00)01527-X

TOPICAL REVIEW

Superconducting bearings

John R Hull

Energy Technology Division, Argonne National Laboratory, 9700 South Cass Avenue, Argonne, IL USA 60439, USA

Received 18 May 1999

Abstract. The physics and technology of superconducting bearings is reviewed. Particular attention is given to the use of high-temperature superconductors (HTSs) in rotating bearings. The basic phenomenology of levitational forces is presented, followed by a brief discussion of the theoretical models that can be used for conceptual understanding and calculations. The merits of various HTS bearing designs are presented, and the behaviour of HTS bearings in typical situations is discussed. The article concludes with a brief survey of various proposed applications for HTS bearings.

1. Introduction

The image of a permanent magnet (PM) stably levitated over a high-temperature superconductor (HTS), as shown in figure 1, is one of the better known icons for HTS technology. This levitation provides a tactile and visual indication of many of the basic phenomena associated with HTSs. If one pushes the PM up, down or sideways, or tries to tilt it, a restoring force returns the PM to its initial position. The forces can also be highly hysteretic. If one pushes hard enough, the equilibrium position of the PM can be changed to almost any orientation or the centre of mass of the PM can be moved to a new equilibrium position. If the PM is a cylinder with a relatively symmetric magnetic field, it readily rotates about its axis of symmetry, as indicated by the blurred arc to the left of the star in figure 1. Such behaviour suggests that the HTS could be used in the construction of a superconducting bearing. In many applications, the advantages of noncontacting surfaces without an active feedback system, ability to operate in a vacuum and potential for extremely low rotational drag should outweigh the inconvenience of refrigerating the HTS. The development of superconducting bearings has progressed significantly since the discovery of HTSs and is reviewed in this article.

While the first stable levitation that involved a superconductor was reported in 1945 [1, 2], it was not until 1953 that efforts to investigate the use of superconductors in bearings and attempts to measure rotational drag were reported [3]. The first experimental motor that employed superconducting bearings was demonstrated in 1958 [4–6]. Despite these and other [7–9] pioneering efforts with low-temperature superconductors (LTSs) that were cooled with liquid helium, significant interest in superconducting bearings did not emerge until the discovery of the first HTS [10]. The discovery was soon followed by a tabletop demonstration of levitation with the new material [11], and shortly thereafter experiments on levitation were reported by many investigators and later reviewed [12–15]. Major advantages of HTSs were their relatively simple fabrication and use in bulk form and a much higher magnetic field before onset of flux-jump instabilities. Although the stable suspension of a superconductor below a PM should have been predictable from magnetization curves as early as 1936 [16], it was only after the experimental demonstration with an HTS [17] that the suspension phenomenon was observed for LTS superconductors at 4 K [18]. The investigation of HTS levitation phenomena was accompanied by early interest in their use as bearings, and small stable rotors with rotational speeds $>100\,000$ rpm were soon demonstrated [19–21].

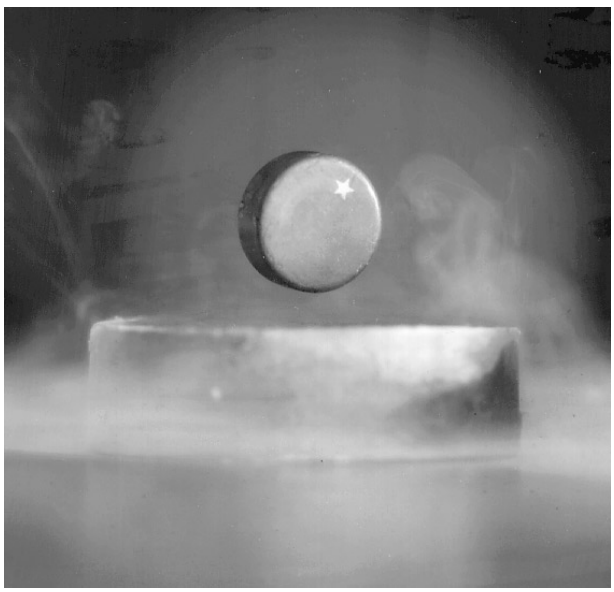

Figure 1. PM (with star) stably levitated over an HTS.

Although the use of wires and thin films in superconducting bearings has been investigated somewhat, most of the current efforts involve the use of bulk HTSs. Whereas in superconducting wire applications, the

supercurrent must pass from grain to grain along a wire length that encompasses many grains, in current levitation applications, it is sufficient that the supercurrent circulate only within individual grains of the bulk HTS material.

The current material of choice for superconducting levitation is Y–Ba–Cu–O (YBCO) and the rare–earth Ba–Cu–O analogues (RE–Ba–Cu–O where RE denotes the rare-earth elements Nd, Sm, Eu, Gd, Dy, Ho, Er, Tm, Yb, Lu, La), because they exhibit a high magnetic irreversibility field H_{irr} at liquid nitrogen temperatures and many have the ability to grow large grains. The H_{irr} marks a phase transition between the region where magnetic flux is solidly pinned in the superconductor and the region where flux may move. Sometimes the H_{irr} curve is said to denote the boundary between the region where flux is frozen and the region where flux is melted. When compared with some of the members of the Bi, Tl or Hg HTS families, YBCO exhibits a relatively low critical temperature of 92 K, but its irreversibility curve is one of the highest at 77 K and lower temperatures. For stable levitation, it is important that the flux be frozen in the superconductor, otherwise, the PM would slowly lose levitation height.

The magnetization of the superconductor is proportional to the product of the critical current density (J_c) and the grain diameter [22]. Large grain diameters are important when sufficiently large magnetizations must be achieved for useful levitation forces. When bulk YBCO materials are made by a melt-texturing process, it is possible to grow grains to diameters of several centimetres [22]. In the present state of the art, the upper limit of the grain diameter produced by this process is ≈10 cm. The ability to produce good-quality YBCO thin films is also limited to approximately this size. If techniques to grow large grains for other HTS materials with high H_{irr} curves could be developed, these materials would also be of interest for levitation applications. Many excellent reviews [23–26] and collected papers [27, 28] cover details of the fabrication issues of melt-textured HTSs. In this review, I will be concerned with HTS properties only insofar as they affect bearing phenomena.

To understand and predict the behaviour of magnetic bearings that use superconductors, one must know the forces that are generated between the superconductor material and a PM or a current distribution. Levitation, suspension, restoring, damping, and drag forces must be determined, and their effect on the dynamic performance of the bearing must be elucidated. Several reviews that describe these forces from a basic physics viewpoint and explore their use in levitation applications have been published [13–15, 29–33]. In this article, I review their application to superconducting bearings.

2. Phenomenology of superconducting levitation forces

A successful superconducting bearing must not only be in equilibrium, but must remain in stable equilibrium when subjected to various perturbing forces at various rotational speeds. This nonlinear dynamics problem requires knowledge of how the magnetic forces and torques change with position and orientation, as well as with linear and rotational velocity.

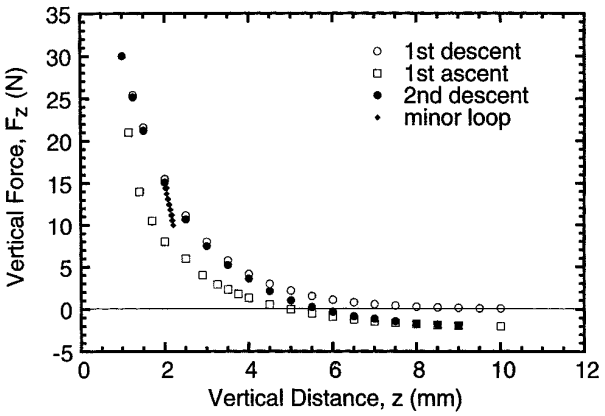

Figure 2. Vertical force against vertical distance between PM and HTS under ZFC.

As discussed in section 4, a very typical geometry for a superconducting bearing is a thrust bearing that consists of a cylindrical PM, with its axis of symmetry and magnetization oriented vertically, that is levitated above an HTS with a flat horizontal upper surface. The diameter of the PM is usually less than that of the HTS. The discussion of forces and stiffnesses in this section is given in terms of this geometry, but the extension of the results to other geometries is usually straightforward.

2.1. Vertical forces

The levitation capability of the PM/HTS system is determined by the vertical force F_z, which is hysteretic for movements in the vertical direction z, as illustrated in figure 2. In this example, a cylindrical, upright, vertically magnetized PM was kept with its bottom surface at a height of 10.0 mm above the top surface of a cylindrical YBCO bulk HTS. For this PM, a separation of 10 mm provides very little magnetic field near the HTS, a situation that is called zero-field cooling (ZFC). After the HTS was cooled in liquid nitrogen, the magnet was slowly brought down to a position 1 mm above the HTS, while F_z was measured at various points along this first descent. The PM was then moved away from the HTS, back to its original ZFC position. Then it followed a second descent, during which a minor reversal of 0.4 mm was effected at a distance of 2.0 mm above the HTS. A second ascent was identical with the first, and a third descent was identical with the second etc.

As seen in figure 2, the force during the first descent is always larger than the force during the second. Upon reversal from 1 mm above the HTS during the first ascent, the force drops very quickly and even becomes negative, indicating an attractive force. A combination of the first ascent and second descent forms a major hysteretic loop, and the area under the curve is equivalent to the hysteretic energy loss. The form of the hysteresis loop leads to the possibility of levitation over a range of heights. For example, if the PM weighed 10 N, equilibrium could exist anywhere in the range of 1.8 to 2.6 mm for the example in figure 2. The PM in this example

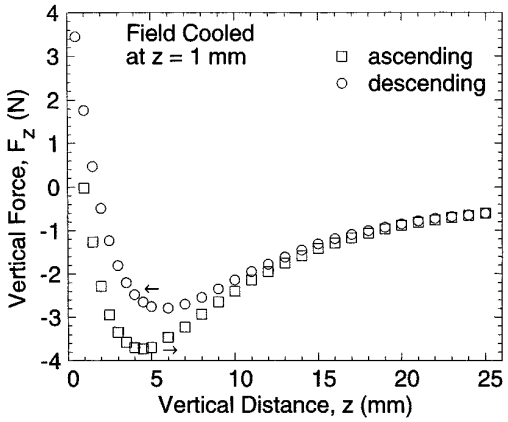

Figure 3. Vertical force against vertical distance between PM and HTS under FC at $z = 1$ mm.

weighed ≈0.02 N, so it is also clear that this type of bearing is capable of supporting a mass many times that of the PM.

Several other aspects of levitational phenomena can be deduced from the curves shown in figure 2. The force is stable in the vertical direction for the case with the PM above the HTS in repulsive levitation, i.e., when z is positive above the HTS, the vertical stiffness $K_z = -\mathrm{d}F_z/\mathrm{d}z$ is positive everywhere. The slope of the minor loop is significantly higher than that determined from the major loop. The stiffness represented by the slope of the minor loop is the dynamic stiffness of the system and would be used to calculate vibration frequencies [34]. The stiffness is positively correlated with the force on initial descent [35], and increases during descent as the separation distance decreases. The width of the minor loop is much smaller than that of the major loop. Thus, the PM/HTS acts as a nonlinear damper, and the damping coefficient increases with vibration amplitude.

A feature of the first descent in ZFC is that for heights less than several millimetres above the HTS surface, the force is exponential with distance [35]. This is probably due to the vertical and horizontal extension of the PM. In practice, it is difficult to measure the force immediately above the HTS, partly because surfaces are not perfectly flat, but mainly because the HTS surface is usually covered with liquid nitrogen. The exponential behaviour allows extrapolation of the force to the surface, and various HTSs can be compared this way if a reference PM of known strength is used. ZFC produces the largest repulsive force but may be impractical, because it requires the cooling of the superconductor before the bearing is assembled.

Hysteresis of vertical force F_z differs significantly when the HTS experiences field cooling (FC), i.e., when the HTS is cooled below its critical temperature while a substantial magnetic field is present, that is, when the PM is close to the superconductor. FC produces less repulsive levitation force than ZFC but can be used to make an attractive-force bearing and generally is more stable in the horizontal direction. An example of the vertical forces experienced after FC is shown in figure 3, where the FC occurred at $z = 1$ mm. The force immediately after FC is almost zero. In principle, there will always be a small amount of repulsive force because of the Meissner effect; however, in practice, this force can usually be neglected because the Meissner fraction for melt-textured YBCO is almost zero [22]. As shown in figure 3, as the PM moves away from the HTS, F_z is negative, indicating that levitation via suspension, with the PM below the HTS, is possible. In this example, the suspension is only stable for $z < 4.5$ mm, where K_z is positive.

The vertical stiffness has been correlated with the vertical force [35], and details of the vertical stiffness have been studied [36–38]. In ZFC, vertical stiffness is approximately independent of descent versus ascent, but slight differences may be observed and are attributed to differing amounts of trapped flux in the HTS during a particular vertical traverse [38]. In FC, the dynamic vertical stiffness is less than, but greater than half, that for ZFC at the same separating distance (i.e. $K_{z,zfc}/2 < K_{z,fc} < K_{z,zfc}$) [38].

The levitation force is approximately independent of the speed at which the PM approaches or recedes from the HTS [29]; however, the measurements can experience force creep. Flux creep is an inherent phenomena in HTSs [12, 29]. A macroscopic manifestation in levitation is force creep, in which the repulsive levitation force decreases with time [39]. For the most part, the force creep is logarithmic in time and can be well correlated with thermally activated flux creep [40]. In this case, it is known that the creep is greater in higher magnetic fields and field gradients (higher levitation forces) but becomes smaller as flux pinning is improved [41]. However, in some experiments with thin films of HTSs, nonlinear force creep that exhibits force jumps has been observed [42].

2.2. Effects of geometry

The geometry and other characteristics of the HTS dramatically influence the levitation force. The levitational force that the superconductor provides is proportional to its average magnetization, which is proportional to the product of its grain diameter times its J_c. Thus, one expects the levitation force to increase as temperature decreases and J_c increases. This is observed experimentally, and the magnetization is well correlated with the levitation force at all temperatures [21]. It is generally believed that the magnetization of the HTS cannot be greater than that necessary to produce a pure diamagnetic image of the PM in ZFC (however, the author has not seen any published proofs for, nor counterexamples to, this conjecture; see also section 3). Thus, beyond a certain J_c or grain size, all HTSs will yield similar bearing pressures, which are determined by the properties of the PM.

The maximum theoretically achievable levitational force is that between the PM and its mirror image. The maximum magnetic pressure P between two uniformly magnetized objects of magnetization M_1 and M_2 occurs at zero gap between the two objects and is given by

$$P = M_1 M_2 / 2\mu_0 \tag{1}$$

where $\mu_0 = 4\pi \times 10^{-7}\,\mathrm{N\,A^{-2}}$. As a convenient reference, for $\mu_0 M_1 = \mu_0 M_2 = 1.0\,\mathrm{T}$, the pressure is 400 kPa. In a sintered NdFeB permanent magnet, $\mu_0 M$ is typically between 1.0 and 1.5 T. The J_c of typical melt-textured YBCO samples at 77 K is ≈40 kA cm^{-2}, which, together with a diameter

of several cm, allows the levitational pressures between the YBCO and an NdFeB PM to reach ≈280 kPa (≈40 psi). Such pressures have been measured in the author's laboratory with very good YBCO samples. However, this pressure occurs at zero separation distance. In a practical system with a finite separation, the pressure will be at least a factor of 2 to 3 times lower.

Although current state-of-the-art melt-textured YBCO is satisfactory for many bearing applications, researchers are continually striving to obtain higher J_c values, partially to more closely approach the theoretical maximum of levitation force, but primarily to improve the economics of using HTS materials in bearings and other applications. Substantially higher J_c values can be achieved by techniques that involve radiation [43], and materials made by these methods are expected to be of interest in bearing designs that require greater magnetic fields and in trapped-flux applications.

The thickness of the HTS is also an important parameter in determining the levitation force. Because the current density is finite, for thin samples the levitation force increases linearly with thickness; however, beyond a certain thickness, the force is mostly independent of thickness [44–46]. This is partially a corollary to the discussion above in that the magnetization in the HTS is limited by the properties of the PM. It is also a result of the inverse-square law of forces between electrical or magnetic poles, in that currents flowing far from a PM will produce a negligibly small force on them.

HTSs are highly anisotropic, with superconducting currents capable of flowing at higher density in the *ab* plane of the crystal. With the ability to grow large single-domain HTSs, the angle dependence of crystal orientation on levitation force has recently been explored [47–50]. For melt-textured YBCO, this anisotropy results in a levitation force that is ≈3 times greater if the *c* axis is parallel to a uniform applied field, than if the *c* axis is perpendicular to the applied field. The force varies monotonically as a function of orientation angle between these two extremes. In actual HTS bearings, the applied field is often some complex combination of parallel and perpendicular orientations that varies over the surface of the HTS.

A number of studies have been performed on the levitational properties of thin-film HTSs [37, 51–54]. Although YBCO thin films often have J_c values of >1 MA cm^{-2} at 77 K, the thickness of these films is only ≈ 1 μm and they do not provide much levitation force. The magnetization quickly saturates, and it is possible to produce very large hysteresis loops if this occurs. However, when unsaturated, the stiffness of such films is often similar to that produced by bulk material of greater thickness [51, 53].

The geometry and condition of the PM also affects the levitation force. The effect of the size and shape of the PM, relative to that of the HTS, has been studied mainly by theoretical models that have been validated by some experimental measurements [54–60]. The magnetization of the PM is temperature dependent, with magnetization increasing with decreasing temperature in most types of PM, but with FeBNd, the magnetization reaches a peak at ≈140 K and then decreases as the axis of easy magnetization changes. In measurements such as those depicted in figures 2 and 3 (where the PM moves in the air) a PM exposed to air will become colder as the distance to the HTS decreases. Unless the temperature of the PM is controlled, the temperature dependence of the PM can affect force measurements and has been known to affect levitation height in HTS bearings [61]. To avoid the complication of PM temperature dependence when forces are measured, it would be possible to keep both the PM and the HTS in liquid nitrogen in ZFC. Because of the temperature dependence of the PM, the procedure would be more problematic in FC, depending on the thermal diffusivities of the PM and HTS. It may be necessary to precool the PM, bring it into the FC position, and then add liquid nitrogen to the system.

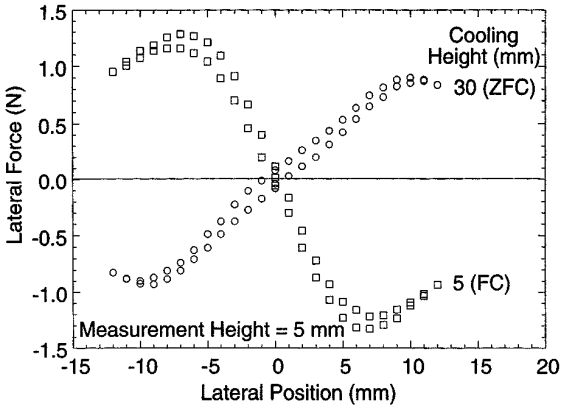

Figure 4. Lateral force against lateral displacement at measuring height of 5 mm in ZFC and FC. Data from [36].

If we assume that the HTS is a single grain of large diameter, then because the magnetization of the HTS is proportional to the diameter of the shielding currents, increasing the diameter of the PM should increase the levitational pressure within some range of the diameter. This effect is expected to saturate once the magnetization of the HTS is approximately equivalent to the diamagnetic image of the PM. The homogeneity of the PM magnetization also affects the levitation force [38] but is mostly relevant in understanding small differences between theoretical models and experimental measurements.

At present, there is no standardized method for measuring or reporting levitation forces. It is tempting to try to relate the measured levitation force to the levitation force produced by a pure diamagnetic image, i.e., the force between the PM and another exactly like it in repulsive levitation. The levitation force is then reported as a percentage of the theoretical maximum [62]. To use this method, one must be careful to appropriately estimate the pure diamagnetic force, and knowledge of the magnetic field only at the surface of the PM is usually insufficient for this purpose [38, 63].

2.3. Horizontal forces

If a PM is moved parallel to the surface of an HTS, the magnetic flux lines are sheared, resulting in a lateral magnetic drag force [29, 64]. This force consists of reversible and hysteretic components. Typical horizontal forces that might be encountered in superconducting bearing applications are shown in figure 4, where the results for a common measurement height of 5 mm and a horizontal traverse from

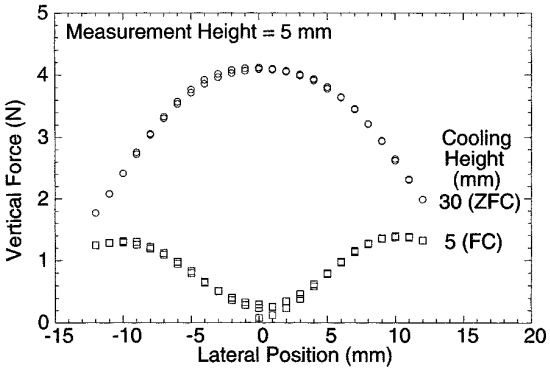

Figure 5. Vertical force versus lateral displacement at measuring height of 5 mm in ZFC and FC. Data from [36].

$x = 0$ to $x = 12$ mm, followed by a horizontal traverse to $x = -12$ mm, followed by a horizontal traverse to $x = 0$ mm, are shown. The figure shows that the behaviour in ZFC is distinctly different from that in FC. For small displacements after FC, the PM is stable, i.e., the horizontal stiffness $K_x = -\partial F_x/\partial x > 0$. In ZFC, the PM is first moved vertically from 30 mm to 5 mm and then lateral traverses are executed. In ZFC, as shown in figure 4, the PM is unstable to horizontal motion, i.e., the horizontal stiffness is negative. In experimental demonstrations in ZFC, the PM may be pushed down almost to the surface of the HTS and then allowed to freely rise to its equilibrium levitation height. Usually, enough flux becomes trapped in the HTS that the levitation is stable, although the horizontal stability is much weaker than in FC. If an HTS is used that exhibits less flux pinning or has smaller grains than melt-textured YBCO, then enough flux may penetrate the system that the horizontal stiffness becomes stabilizing even in ZFC. Of course, the levitational force will also be lower. For the system shown in figure 4, edge effects of the HTS produce the force maxima. In FC, if a smaller-diameter PM is used, the force maximum becomes a plateau and the result is a constant drag force for continued horizontal motion in the same direction [64].

One may show both experimentally and analytically that in FC, the horizontal stiffness is exactly half the field-cooled vertical stiffness (i.e., $2K_{x,fc} = K_{z,fc}$) [38]. This forms an interesting analogue to the stiffnesses as determined by Earnshaw's theorem for magnetic systems (see section 2.7), in which $2K_x = -K_z$. In the PM/HTS system in FC, all of the stiffnesses are positive.

2.4. Cross stiffness

The PM/HTS system exhibits an anisotropic form of cross stiffness, which has only recently been investigated [38, 65, 66]. If the PM moves in the vertical direction, horizontal force is negligible. However, if the PM moves in the horizontal direction, the magnitude of the vertical force can change, as shown in figure 5, where the lateral traverse is the same as in figure 4. As in the case with horizontal forces, there is a difference in the sign of the cross-stiffness term, depending on whether the system was in ZFC or FC.

2.5. Nonlinearity of forces

For superconducting-bearing applications, where the expected vertical or horizontal vibration amplitudes are typically < 1 mm, the forces in the PM/HTS interaction can be divided into an elastic region that occurs at small amplitudes, and a hysteretic region that dominates for amplitudes that are larger than some threshold. In the elastic regime, the flux lines remain in their pinning centres, bend as the PM moves, and produce a restoring shear force, according to the Maxwell electromagnetic stress tensor. The hysteretic regime begins when the PM moves sufficiently far for some flux lines to move from their original pinning centres to new ones.

In the hysteretic regime, the force is nonlinear and has been compared with dry friction in mechanical problems [15, 27]. For an HTS with an incomplete penetration of magnetic field, the energy dissipation E_h in a complete hysteresis cycle is [22]

$$E_h = A(\Delta B)^3/J_c \tag{2}$$

where A is a geometric factor of order unity and ΔB is the peak-to-peak variation of the magnetic field. Because ΔB is approximately proportional to the displacement of the PM, the energy loss is approximately proportional to the cube of the amplitude, and the friction force is amplitude dependent and nonlinear.

The manifestation of the elastic/hysteretic behaviour occurs in many parameters that affect superconducting bearings. The vertical and horizontal stiffnesses are dependent on the amplitude of vibration [67, 68]. For small amplitudes, the stiffness is constant, but, after some critical amplitude that depends on levitation height, the stiffness begins to decrease as the amplitude increases. The higher the current density of the superconductor, the higher the critical amplitude value for the onset of stiffness decrease. A transition between elastic and hysteretic behaviour has also been observed in the width of minor loops in the force measurements [69]. The decay of oscillations from PMs, either freely levitated [70, 71] or attached to vibrating beams [72], is another method used to study this transition. The hysteretic loss is mostly frequency independent. However, detailed studies of losses in PM/HTS systems and superconducting bearings show the presence of small velocity-dependent effects that appear to be intrinsic to the superconductors [73–75].

2.6. Vibrating systems

A superconducting bearing will undergo vibrations at various frequencies during its operation. The study of stiffness and damping in vibrations of PM/HTS systems has been alluded to above. The damping characteristics of YBCO near 77 K are highly temperature dependent [76], and it has been suggested that this feature be used as a switchable damper, which seems particularly attractive for HTS films [77].

The vibrations of a PM near an HTS have been shown to produce period doubling and chaos [78]. Another route to chaotic vibration is bifurcation of quasi-periodic oscillations [79], and in this case multifractality appears in the critical state of chaotic motion [80].

2.7. Stability

To appreciate the stability of the PM/HTS system, one need only compare it with most other passive magnetic systems, which are statically unstable. Most magnetic systems are governed by Earnshaw's theorem, which states that there is no stable, static three-dimensional arrangement of a collection of poles (electric, magnetic, or gravitational) whose magnitudes do not change and which interact via a $1/r^2$ force law [81]. Particles that experience inverse-square-law forces obey Laplace's equation, and Earnshaw's theorem is developed from the property of the associated curl- and divergence-free fields that precludes the existence of local, detached, scalar-potential maxima or minima, and allows only saddle-type equilibria. In terms of magnetic stiffness K, the theorem for a collection of poles can be written as

$$K_x + K_y + K_z = 0. \tag{3}$$

For axisymmetric systems, the theorem may be rewritten as $2K_x = -K_z$, and the system will be unstable in the direction that exhibits the negative stiffness. Braunbek extended Earnshaw's result to show that electric or magnetic suspension is not possible when all materials have $\varepsilon_r > 1$ or $\mu_r > 1$, but that it is possible when materials with $\varepsilon_r < 1$ or $\mu_r < 1$ are introduced (where ε_r is the relative electrical permittivity and μ_r is the relative magnetic permeability) [82]. These results collectively are often referred to as Earnshaw's theorem.

Although superconductors probably do not strictly satisfy most formal definitions of a diamagnetic material ($\mu_r < 1$), the HTS often strongly mimics the behaviour of a pure diamagnetic material ($\mu_r \ll 1$), and it is useful to invoke this picture when we strive to understand many of the levitational phenomena. Diamagnetic materials, such as superconductors, are not governed by Earnshaw's theorem, and they enable the possibility of creating stable levitation systems.

3. Modelling

One of the fundamental properties of superconductors is their tendency to exclude magnetic flux from their interiors. Accordingly, a superconductor with a PM positioned close above it, as shown in figure 6(a), develops a shielding current that excludes flux and causes the actual magnet to 'see' its mirror image in the ideal case. Over a flat superconducting surface, the PM is stable in the vertical direction. Horizontal stability is obtained if the superconductor is given a concave shape, so that vertical superconducting walls are formed around the PM, as first demonstrated with lead, a type-I superconductor [1, 2]. The shielding currents in a type-I superconductor are completely loss free, so that, in the absence of viscous drag from surrounding gas or eddy currents or hysteresis in the PM, oscillations of a PM above a type-I superconductor will be undamped.

In type-II superconductors, the stability of the levitational phenomena that is a result of the diamagnetic response is greatly enhanced by the additional phenomena associated with flux pinning. When sufficient flux lines are

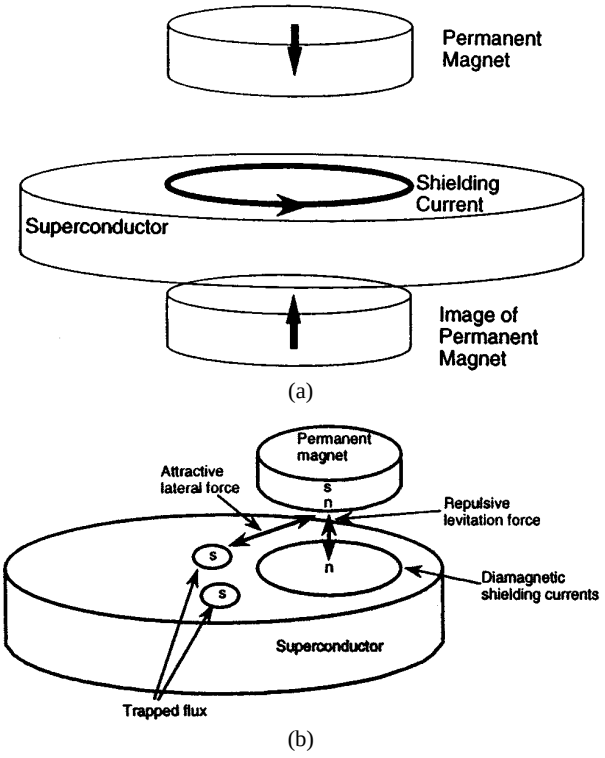

Figure 6. Schematic diagrams of conceptual levitation models: (a) diamagnetic response, (b) flux trapping.

trapped in the HTS, the PM remains levitated in position, even over a flat surface. If the flux pinning is sufficiently strong, the magnet can be stably suspended below the superconductor, or even along its side. The flux lines between the PM and the HTS act in an imperfect analogy to mechanical springs with attachments on the PM and in the HTS. If the PM moves a small distance laterally, so that the flux lines still remain in their pinning centres, the flux lines bend and produce a laterally restoring shear force, according to the Maxwell electromagnetic stress tensor. If the PM moves vertically or horizontally, the 'springs' pull the magnet back to its equilibrium position.

If the PM moves far enough laterally that the flux lines move from their original pinning centres to new ones, an additional stabilizing force that involves additional trapped flux begins to act. The moving flux lines induces additional supercurrents, and the associated additional trapped flux forms regions of induced magnetization in the superconductor of the same pole orientation as the levitated magnet, which decreases the local flux. As shown in figure 6(b), the result is an attractive interaction with the permanent magnet that provides a lateral restoring force. Because the additional trapped flux remains in the original location, the lateral motion of the PM produces a slight increase in the vertical force.

Although flux pinning is most prominently associated with FC, strong flux pinning near the HTS surface can greatly extend the range over which the HTS behaves almost like a pure diamagnetic material in ZFC.

3.1. Critical-state model

The critical-state model [83, 84] is often invoked to explain many of the levitational phenomena [85–97]. While calculationally cumbersome in many bearing geometries, it is rooted in a physics that contains the essential features of flux pinning in type-II superconductors and has been used successfully for many years to analyse ac losses and flux jumping in low-temperature superconductors and HTSs. In a critical-state model, one often assumes that at any location in the superconductor, the current is either flowing with magnitude J_c or is zero. J_c may be assumed constant or assigned a dependence on magnetic field. The critical-state model has had good success in characterizing many of the hysteretic behaviours of HTSs in levitational situations.

In HTSs that are composed of small grains, some models assume that the grains may be treated as cylinders and that the magnetic field propagates from the cylinder wall to the interior [86, 90]. Other models calculate the performance under the assumption that the grains are completely penetrated [92]. If the more physically correct model of a J_c that depends on magnetic field is used, it is important to take into account the actual internal magnetic field of the HTS, which includes effects of self-demagnetization. How the supercurrents distribute themselves in the HTS is usually somewhat arbitrary in the models. In ZFC for large-grain HTSs, models usually assume that the shielding currents begin at the surface [97], although recent efforts have investigated the use of thermal annealing algorithms to calculate the J_c distribution *ab initio* [96]. In the axisymmetric cases investigated with most models, it is usually assumed that the *ab* plane of the HTS is horizontal and that the current flows exclusively in these planes.

3.2. Image models

In many cases in which hysteretic behaviour is not important, the HTS can be treated as a pure diamagnet and the PM as a set of magnetic dipoles. As in figure 6(a), a diamagnetic image is formed in the superconductor, with each magnetic dipole of the PM represented by its mirror image dipole that is oppositely magnetized and located the same distance below the superconductor surface as the magnet is above the surface. As the PM moves closer to or further from the superconductor surface, the distance of the image changes accordingly. The calculation of levitation force often reduces to that between a PM and its mirror image. The advantage of this approximation is that analytical solutions are available for a number of geometries [98–101]. The model can be readily adapted to finite-element calculations by setting the relative permeability of the HTS to a very small value, and the effects of flux penetration can be finessed in a crude approximation by allowing the relative permeability to take on some finite value that is less than unity [55, 102]. These pure diamagnetic models do not allow for the calculation of dynamic stiffness or any losses.

A model that combines a 'frozen' mirror image [103] with the diamagnetic mirror image may be used to describe many of the dynamic stiffness properties in FC [104]. In this model, two images appear in the superconductor: a diamagnetic image of the PM that follows the movement of the PM, and a frozen image that is equal in magnitude and location to the diamagnetic image at the time of FC but oppositely polarized and remains in its initial location even if the PM moves. The frozen-image model can be used to provide a good intuitive conceptualization of the relationship between lateral and vertical stability. In particular, it explains why, even if infinite pinning strength were present in the superconductor, there would be a finite lateral stiffness. Comparison of the predictions of this model with experimental results shows that, for PM movements of less than several millimetres over a melt-textured HTS, the forces and stiffnesses agree well enough to be useful in most HTS bearing calculations [38]. If the HTS can be treated as having infinite horizontal extent, then the frozen-image model also provides a good quantitative description of the stiffnesses; however, in real systems with finite HTSs and PMs with spatial extent, the three-dimensional geometry and edge effects will complicate the calculation, especially for lateral stiffness in ZFC [38]. As in the pure-diamagnetic model, the frozen-image model does not predict effects associated with hysteresis.

4. Bearing designs

In the most common configuration for a basic HTS bearing design, the PM is levitated and free to rotate while the HTS is held stationary. This is mostly due to the convenience of cooling the HTS in boiling liquid nitrogen or by a good thermally conductive contact with a cold source. If the bearing is to operate in vacuum, the only heat transfer mechanism for the levitated component is radiation, which is governed by Stefan's law, and losses are very low at cryogenic temperatures. Because the Curie temperature of commercially available PMs is significantly higher than the critical temperature of HTSs, the configuration in which the PM is levitated exhibits the greatest thermal stability. In situations where the bearing application allows gaseous cooling, or even circulation of a liquid cryogen, it may be preferable to hold the PM stationary and allow the HTS to levitate and rotate.

The two basic rotating bearing types are thrust and journal. In a thrust bearing, the major load force is in the direction of the rotational axis; in a journal bearing the load force is perpendicular to the rotational axis. A typical PM/HTS journal bearing configuration could consist of a rotating shaft with PM discs mounted as endcaps, and the shaft assembly supported by HTS bushings that completely or partially surround the PMs at both ends of the shaft assembly. The arrangement shown in figure 1 is an example of a journal bearing. In this review, the discussion focuses almost entirely on the thrust type, either of the repulsive or attractive configuration. Researchers have also demonstrated PM/HTS journal bearings [19, 29, 105], and much of the discussion here is directly applicable to this type of bearing.

One may classify a magnetic bearing as either a levitation bearing, which is expected to provide a mostly constant force, or as a stiffness bearing, which provides a stabilizing force against disturbances and for which the average net force is zero. Most practical magnetic bearings are often a combination of levitation and stiffness type. In a magnetic

levitation bearing, the thrust bearing has a significant advantage over the journal bearing. To provide a levitation force, the magnetic pressure must be greater at the bottom of the levitated component than it is at the top. The magnetic pressure P is determined by the Maxwell stress tensor as

$$P = (B_t^2 - B_n^2)/(2\mu_0) \tag{4}$$

where B is the magnetic field along the plane on which the pressure is to be determined, subscript t denotes the component that is tangential to the plane, and subscript n denotes the component that is normal to the plane. Therefore, a system with a levitation force must experience a different magnetic field at the top than it does at the bottom. In a journal bearing, the rotating component experiences the difference in magnetic field on every part of the perimeter during each rotation; this produces eddy currents and hysteretic losses. In a levitational thrust bearing, the magnetic field remains the same on the top and bottom horizontal surfaces during the rotation, unless there is some azimuthal inhomogeneity in the PM or HTS. The use of nonconducting ferrite PMs would eliminate the problem of eddy currents in journal bearings, but the available magnetization of these materials is significantly lower than that of FeBNd or SmCo, and the levitation pressures obtainable are thus much lower. In a pure stiffness bearing, there is usually no advantage of a thrust over a journal type.

To maximize the levitation pressure in a PM/HTS system, one may increase the magnetic field at the bottom of the PM by making the PM cylinder taller. This has the disadvantage of increasing the levitated mass and cost of the PM. A more acceptable design uses nested rings of PMs with alternating vertical polarity and includes a shunt of soft-ferromagnetic material on top of the rings [106, 107]; radially magnetized nested rings separated by soft ferromagnets are also possible. Several studies have addressed the optimization of these designs [108–111].

In practical HTS bearings, the low levitational pressure available in the interaction between the PM and the HTS is often augmented by various hybrid schemes in which interactions between pairs of PMs provide the bulk of the levitational force. These methods are sometimes termed magnetic biasing. The PM/PM interactions are statically unstable, as Earnshaw's theorem predicts, but the inclusion of a properly designed HTS component in the bearing is sufficient to stabilize the complete bearing. Among the advantages of magnetic biasing are that less mass of PM must be levitated and much less HTS must be cooled. Three of these augmentation methods are shown in figure 7.

Figure 7(a) shows augmentation in the form of an Evershed-type design [61, 112, 113]. Here, the levitated rotor consists of a levitation PM, below which hangs a rigid rod with a smaller stabilizing PM on the bottom. The levitation PM of the rotor experiences an attractive force toward the stator PM immediately above it. This system is statically stable in the radial direction but unstable in the vertical direction. The gap between the levitation PM and the stator PM is adjusted in such a manner that the attractive force between the pair of magnets is just less than 100% of the rotor weight, so that the rotor would tend to fall. The remainder of the weight is provided by the interaction between the stabilizing PM and the HTS; this interaction also supplies sufficient stiffness for vertical stability and some additional radial stability.

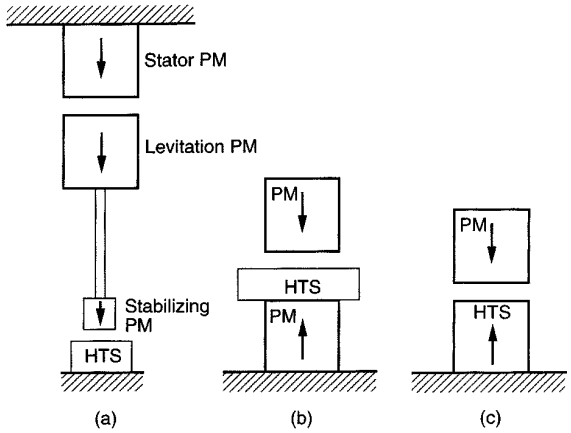

Figure 7. Magnetic biasing methods to improve the levitational pressure in HTS bearings: (a) Evershed-type design with attractive-force augmentation, (b) repulsive-force augmentation and (c) trapped-field augmentation.

Figure 7(b) shows augmentation in which a stator PM is placed below the HTS and acts in repulsion with the levitated PM [113]. Here, the PM/PM interaction is vertically stable but horizontally unstable. Because the minimal separation distance between the two PMs is limited by the thickness of the HTS, the amount of augmentation in this particular configuration is somewhat limited. Various combinations of attractive-force and repulsive-force hybrids have been devised [113–115].

Another method to augment the levitation pressure is to use trapped fields in the HTS [116], as shown in figure 7(c). To create trapped flux, the HTS is usually field cooled in the presence of an external electromagnet or superconducting magnet. Alternatively, large pulsed fields can be applied after the HTS is cooled, although this method is the less effective of the two at trapping flux. The reported trapped fields are usually the maximum value measured at the surface of the HTS after the magnetizing fields have been removed. The average magnetization of the cylindrical HTSs is significantly less than these maximum fields. Trapped fields that are significantly >1.0 T have been reported at 77 K, and fields of up to 10 T have been reported at lower temperatures [116–119].

The diameters of high-performance melt-textured HTSs are currently limited to a maximum of $\approx$100 mm. A large bearing system will thus need an array of superconductors [120]. In the case of a single magnet levitated over an array of superconductors, an additional loss arises from magnetization of the individual superconductors upon levitation. The magnetization of the array leads to an ac magnetic field that is seen by the rotating PM, and to eddy current losses that depend on the electrical conductivity of the PM [61, 121]. These losses can be minimized by appropriate use of one of the augmentation designs [61].

One of the advantages of noncontact in magnetic bearings is elimination of overheating as the determining factor for the maximum speed of the bearing. Instead, the

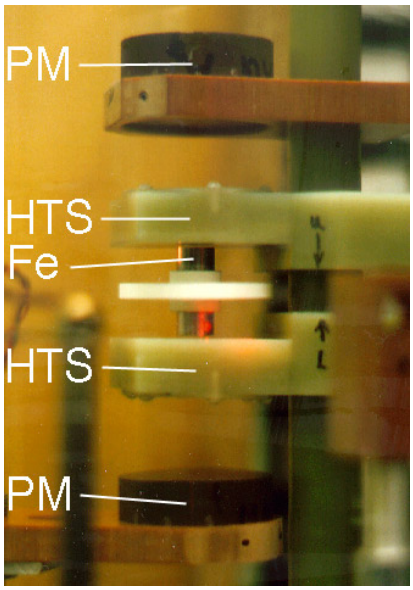

Figure 8. Mixed-μ HTS bearing.

speed of the bearings tends to be limited by the mechanical strength of the rotating bearing components. PMs and HTSs are brittle and exhibit low mechanical strength, both of which lead to structural failure under sufficiently large centrifugal forces. These materials can be radially banded by materials with greater tensile strength, however, designs that allow for high velocities at the bearing perimeter require a careful balance between mechanical strength and the requirements of the magnetics [106, 122].

An alternative design to the conventional PM/HTS system is the mixed-μ bearing [123, 124], shown in figure 8. In this bearing, a soft ferromagnetic cylinder (Fe) ($\mu_r > 1$, where μ is the relative magnetic permeability) is levitated in attractive levitation between two PMs and stabilized by two HTSs ($\mu_r < 1$), one HTS placed between the rotor and each of the PMs. The PM pair induces a magnetization in the Fe, which experiences a levitation force that depends on the gradient of the applied magnetic field from the PMs. For stabilization, the magnetization induced in the Fe produces diamagnetic images and trapped flux in the HTSs. In figure 8, the HTSs are housed in nonmetallic cryochambers, the lower PM is mounted on a movable stage and the Fe cylinder is surrounded by a ceramic disc-type rotor. The PMs shown in figure 8 are approximately identical, and, in this case, to obtain a net upward force, the distance between the upper PM and the rotor must be less than the distance between the lower PM and the rotor.

One advantage of this design is that the rotor can be made of a material with high tensile stress, such as steel, and its maximum rim velocity should be significantly greater than that for a rotating PM or HTS. A second advantage is that losses in the HTSs are not affected by inhomogeneities in the PMs. The primary contribution to a changing magnetic field near the HTSs is due to radial oscillation of the rotor. To date, the mixed-μ bearing has displayed the lowest rotational loss of any HTS bearing tested in the author's laboratory. Disadvantages of the mixed-μ design include a stability that is weaker than the stability of the PM/HTS configuration and difficulty in scaling the design to larger sizes.

Several researchers have investigated the possibility of combining HTS bearings with active magnetic bearings [125–128] and with eddy current dampers [129]. Another design possibility is the levitation of a bulk HTS with a stationary coil that is either an electromagnet or, preferably, a superconducting magnet [130–133]. A major advantage of this approach is a higher levitation pressure, in that ferromagnetic materials may achieve magnetizations up to $\approx$2.5 T, and, with an NbTi superconducting coil, the magnetic field at the surface of the HTS can easily be 5 T. A further advantage is that azimuthal homogeneity of the magnetic field produced by a coil can be much higher than that attainable in a PM; therefore the potential for extremely low-loss bearings exists. To take advantage of the homogeneity, it would be necessary to hold the energizing current of the coil constant in time to prevent changes in levitation height. The main disadvantage of this approach, when compared with levitating a PM, is that much lower temperatures are required and the levitated HTS must be cooled over long periods of time.

5. HTS bearing phenomena

The parameters needed to characterize a bearing for use in rotating a mass are the levitational force, dynamic stiffness, damping, and rotational loss. The 280 kPa levitational pressure of an HTS bearing is lower than that achievable with a conventional electromagnetic bearing ($\approx$1 MPa) and significantly lower than that typically achieved with mechanical roller bearings ($\gg$10 MPa). However, even in the present early period of technological development of superconducting bearings, several laboratories have stably levitated and rotated masses >200 kg. In principle, the amount of mass that can be levitated is limited only by the number and size of PMs and HTSs that are available.

5.1. Rotational loss

The ease with which a PM disc spins when levitated over an HTS, and the absence of contact between the surfaces, produce the illusion that the rotation is lossless. In reality, small magnetic losses gradually slow the rotation. These losses are primarily the result of azimuthal inhomogeneities in the magnetization of the PM disc, which produce hysteretic loss in the superconductor. Typically, for PMs with the best homogeneities, the amplitude of the ac component of the magnetic field at a fixed radius above the rotating surface is $\approx$1% of the average field at that radius. Although small, this inhomogeneity is sufficient to cause a detectable decay in rotational rate when the magnet spins in vacuum.

A figure of note for the rotational decay of a bearing is the coefficient of friction (COF), defined as the rotational drag force divided by the levitational force (weight of the levitated rotor) [123]

$$\mathrm{COF} = -(2\pi R_\gamma^2 \mathrm{d}f/\mathrm{d}t)/(gR_D) \qquad (5)$$

where R_γ is the radius of gyration of the rotor, f is the rotational frequency, t is time, g is the acceleration of gravity

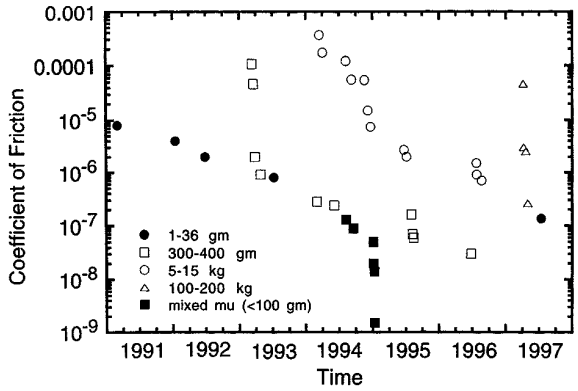

Figure 9. History of lowest COF attained when using HTS bearings for low-speed rotors at Argonne National Laboratory.

and R_D is the mean radius at which the drag force acts. In equation (5), all terms are easily measured or calculated except R_D, the value of which is somewhat ambiguous because, *a priori*, we do not know the bearing loss mechanism nor how it is distributed over the radius of the bearing. To be definitive, the author always takes R_D to be the outer radius of the bearing part of the rotor.

The COF is useful when comparing the performance of different bearing designs or designs that use various types of HTS because it helps to normalize the effects of bearing size and differences in moment of inertia (R_γ term) among experimental devices. The COF for a mechanical roller bearing is of the order of 10^{-3}. The COF for an active magnetic bearing is $\approx 10^{-4}$ when parasitic losses for the feedback circuits and power for the electromagnets are factored in. Measured COFs for simple HTS bearings are as low as 10^{-7}. The parasitic losses of a superconducting bearing are due to the power that is required to keep the superconductor cold. For refrigerators that operate at ≈30% of Carnot efficiency (the theoretical maximum) ≈14 W of electricity are required to remove 1 W of heat at liquid nitrogen temperatures. Thus, the equivalent COF for an HTS bearing with parasitics factored in is $\approx 2 \times 10^{-6}$, about two orders of magnitude lower than the best alternative bearing. To accurately measure the low COF values that can be attained with HTS bearings, chamber pressures must be $\lesssim$1 MPa to reduce air friction [134]; however, for most practical applications, the vacuum requirement is not so stringent.

Figure 9 shows the historical reduction in attainable COF for various types of HTS bearing at the author's laboratory. Similar progress has occurred at other laboratories in the world. The 1–36 g category represents a single PM disc levitated over a single HTS, and the progress in reducing the COF here is mainly due to continual improvements in increasing J_c and grain diameters and to improving the alignment of the c axis in melt-textured YBCO, as was demonstrated in one of the first studies of rotational decay in HTS bearings [135].

The 300–400 g category represents a single-piece PM ring levitated over an array of HTSs. Progress in reducing COF here can be attributed to optimizing the array geometry and better understanding of the cryochamber design [121], methods for improving the homogeneity of the magnetic field of the single-piece PM ring [134], and to effective use of an Evershed-type design [61]. Starting at a speed readily attainable without mechanically reinforcing the PM ring, this type of bearing should be able to continuously rotate for more than 10 years before coming to rest.

The 5–15 kg category represents a double ring composed of PM segments and levitated over an array of HTSs. Progress in reducing the COF in this category is mostly due to developing better construction techniques for the PM rings [106, 122], as well as continued improvements in the properties of the HTSs.

The 100–200 kg category represents a combination of PM/HTS bearings in an Evershed-type design. The mixed-μ bearing was discussed in the previous section. The progress exhibited in figure 9 demonstrates that low rotational losses can be achieved in a wide variety of bearing types and that size does not seem to be a limit on attaining low COFs.

5.2. Bearing dynamics

The low stiffness of the HTS bearing has profound consequences in rotor dynamic behaviour that are not exhibited with other types of bearing. Rigid-rotor bearing resonances, due to the magnetomechanical interactions in the PM/HTS system, occur at very low frequencies of the order of several hertz. Thus, the operating speed regime of disc or ring-type rotors is in the supercritical range, well above the bearing resonant frequencies. The frequencies are determined by the dynamic stiffnesses of the system and will generally involve some combination of FC and ZFC effects. Following the same trend as the stiffness, the resonant frequencies decrease with increased separation between PM and HTS. For a given bearing design, however, the frequency is mostly independent of the bearing load, with an increase in load producing a decrease in separation that increases the stiffness to mostly compensate for the increase in mass [136]. As a result, there is usually a large operating speed range between the bearing resonances and the frequencies at which bending modes start to appear in the rotor structure. Further, the low-stiffness bearing allows the rotor to self-centre at low speeds, with relatively low out-of-balance forces at these resonances, so rotor balancing is less critical than with other bearing designs.

The HTS bearings often contain large gaps between rotating and stationary surfaces and are capable of tolerating radial oscillations of several millimetres in amplitude. The hysteretic nature of a superconducting bearing makes damping of translational motion amplitude dependent. For low-amplitude vibrations, damping is small, but it quickly increases as vibrational amplitude increases. The hysteretic nature also leads to a greater uncertainty of the equilibrium position of the rotor than is typical in most rotating machinery, and this also requires larger running clearances. Before the HTSs are cooled, the bearing is statically unstable, as predicted by Earnshaw's theorem. Thus, some mechanical constraint is necessary before and while the HTSs are cooling, and this constraint must be removable after cooling for a contact-free levitation.

Two synchronous resonances occur in a magnetically suspended rotor with a polar moment of inertia greater than

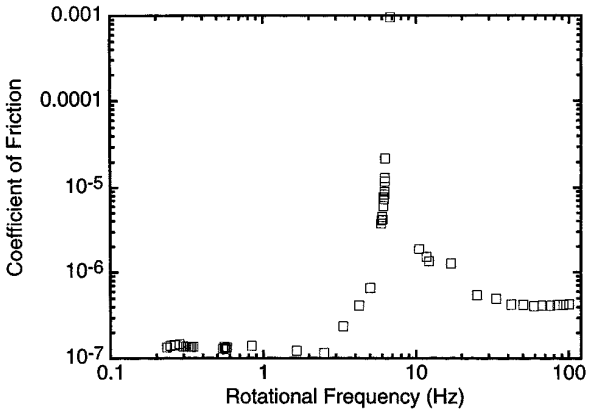

Figure 10. COF against rotational frequency for a 25.4 mm diameter, 9.6 mm high PM disc levitated 10 mm above a YBCO cylinder.

the transverse moment (i.e., a disc geometry): one is vertical and one is radial. Based on the ratio of HTS levitational and horizontal dynamical stiffnesses, one expects the frequency of the vertical mode to be higher than the frequency of the radial mode. At a given rotational frequency, the COF is positively correlated with the amplitude of vibration [124]. In practice, the radial mode has the largest effect on the COF in most HTS bearing systems. Usually, a vibration amplitude at the natural frequency of the radial mode is present at all rotational speeds; however, the amplitude greatly increases when the rotational frequency is close to that of the natural radial frequency [124].

Figure 10 shows the COF as a function of rotational frequency for a disc PM that is levitated 10 mm above a single YBCO cylinder and spinning in a vacuum chamber. The behaviour shown in figure 10 is typical for most HTS bearing designs in which rotors have disc-type moments of inertia and in which eddy currents have been nearly eliminated. One may divide the behaviour into three regions: below the resonance, at the radial resonance, and above the resonance in supercritical operation. Below the resonance ($f < 3$ Hz), the levitated structure rotates about the centre of magnetism of the bearing, and the losses are caused by the inhomogeneity of the PM's field. The resonance region (3–20 Hz) shown in figure 10 is relatively broad and probably includes some coupling to the vertical vibration mode. The large COF value is mainly caused by the large-amplitude radial oscillations in this frequency range. In some systems, especially those with well balanced rotors, the resonance is very narrow, and the vertical mode, if present at all, contributes very little [134].

Above the resonance (>20 Hz), the losses are affected by an additional factor, which is caused by the rotation of the magnet about its centre of mass rather than its centre of geometry or centre of magnetism. This transition of rotation centre in passing through a resonance is well understood in Jeffcott-rotor theory [137]. The rotation about the centre of mass produces a whirling motion of the centre of magnetism over the HTS, and the additional hysteresis loss is proportional to the radial gradient of the magnetic field of the PM and the amount of offset of the centre of mass from the centre of magnetism. This factor has been modelled by assuming the bearing is a linear, elastic, isotropic spring with structural damping [138]. As shown in figure 10, above and below the resonance, the losses are mostly independent of velocity. However, detailed studies of losses in HTS bearings show the presence of small velocity-dependent effects that appear to be intrinsic to the HTSs [73–75]. If the rotor is in perfect balance, the COF above and below the resonance will be identical.

For a more generic rigid rotor, such as a long PM cylinder levitated over a HTS, there are six possible modes of vibration. These modes may be excited by external vibrations, e.g., the motion of the earth vibrating the HTS, or by synchronous excitation as the rotational frequency of the PM coincides with a vibrational mode frequency. In an axisymmetric system, the six modes usually degenerate into four frequencies: a very low (usually sub-Hz) rotational frequency about the axis of symmetry that can usually be ignored, a vertical oscillation of the mass centre, a radial oscillation of the mass centre (two degenerate modes) and a tilt of the axis of symmetry about the vertical axis (two degenerate modes). All of the modes are typically detectable when the PM is levitated and not rotating. All of the modes are somewhat dependent on rotational frequency, especially the tilt mode. If the transverse moment of inertia of the rotor is greater than its polar moment, there is an additional synchronous resonance, which exhibits the form of a conical vibration, i.e., the top of the rotor moves to one side while the bottom of the rotor moves to the opposite side. The frequency of the conical mode depends on the rotational frequency, and this type of rotor never truly enters the supercritical range, but rather the ratio of rotational frequency to conical-mode vibrational frequency approaches an asymptotic limit that depends on the ratio of the moments of inertia.

A phenomenon related to bearing dynamics is the possibility for self-oscillation that may lead to rotation of a PM disc initially levitated without motion over a HTS [29, 139, 140]. The cause of the phenomenon appears to be a temperature gradient across the PM, in which the temperature dependence of the magnetization causes the centre of levitation force to reside below the centre of gravity, a situation that is mechanically unstable. If the oscillation frequency and the thermal diffusion times in the PM are appropriately matched, small oscillations can grow into larger amplitudes and eventually become a self-sustaining rotation.

A completely different phenomenon that also affects an HTS bearing is the need for a larger breakaway torque at startup than is required to keep the bearing rotating at constant speed [141]. This phenomenon, which is believed to be due to the azimuthal inhomogeneity of the PM, is analogous to the difference between static and dynamic friction in mechanical systems. An expected corollary to this phenomenon, and one that has been observed experimentally, is the observation that the drag torque is not constant as a function of rotation angle [142].

The dynamics of HTS bearings under the influence of the inherent nonlinear forces are still actively studied [65, 143]. The cross-stiffness term in which the vertical force varies with radial displacement has been shown to cause a bifurcation of the solution for steady-state motion near the resonance [66], a prediction that has been verified by COF measurements [38]. A ramification of this result is that the torque needed to

continue acceleration of the rotor requires a substantial step increase at a frequency slightly below the resonance peak. The precession of the levitated PM and the decay of tilt angle after disturbances have also been studied [144].

Another dynamics topic of critical relevance to the operation of HTS bearings is the change in levitation height caused by a varying magnetic field at the surface of the HTS, either from radial vibrations or pure rotation of the PM. An early work reported that the application of an ac field could produce a unique levitation height of an HTS levitated above a ring-shaped PM, independent of the initial height anywhere in the region allowed by the hysteresis loop [145]. An applied ac field was also observed to be capable of changing the orientation of a levitated HTS [146].

A drift in levitation height under either a variable magnetic field or a vibration has been studied by several researchers [147–154]. Such a drift is in addition to any possible change in levitation height due to force creep. The drift in levitation height can be made so severe that levitation is totally lost [152–154], but these extreme cases can usually be avoided by proper bearing design. In the many experiments performed in the author's laboratory, some rotors have experienced a drop in levitation height of several hundred micrometres immediately after passing through the resonance, but after operation at higher speeds this gap is usually recovered.

6. Applications

Because superconducting levitation is versatile over a wide range of stiffness and damping, it has been suggested for numerous applications [29]. Superconducting bearings, like magnetic bearings, do not require a lubricant; this could be a major advantage in harsh chemical or thermal environments. In addition to the early applications considered for low-temperature superconductors mentioned in the introduction, such as electric motors and gyroscopes, our increased understanding of the hysteretic behaviour of HTSs has suggested new possibilities.

The availability of HTS bearings that are so nearly friction-free naturally leads to their consideration for flywheel energy storage, and several major projects have investigated this application [31, 120, 127, 155–159]. Flywheels with conventional bearings typically experience high-speed idling (that is, no power input or output) losses of the order of $\approx$1% per hour. With HTS bearings, it is believed that losses as little as 0.1% per hour are achievable, even when the flywheel powers the refrigerator that cools the HTSs. When coupled with efficient motors/generators and power electronics (capable of losses as low as 4% on input and output), the potential exists for constructing flywheels with a 90% diurnal storage efficiency. Probably only one other technology is capable of achieving such high diurnal storage efficiencies: large superconducting magnetic energy storage, which employs superconducting coils hundreds of metres in diameter.

Electric utilities have a great need for efficient diurnal energy storage, such as flywheels, because their inexpensive baseload capacity is typically underutilized at night and they must use expensive generating sources to meet their peak loads during the day. A distributed network of diurnal-storage devices could also make use of underutilized capacity in transmission lines at night and add robustness to the electric grid. These factors are expected to become more important in the forthcoming deregulation of the electric utility industry. Efficient energy storage would also be beneficial to renewable energy technologies, such as photovoltaics and wind turbines.

With modern graphite fibre/epoxy materials, the inertial section of a flywheel rotates with rim speeds well in excess of 1000 m s^{-1} and achieves energy densities greater than those of advanced batteries. The kinetic energy in a (large) Frisbee-sized flywheel with this rim speed is $\approx$1 kW h, and a person-sized flywheel could store 20–40 kWh. Experimental versions of flywheels that employ HTS bearings have already stored $>$ 2 kWh.

HTS bearings are particularly interesting for cryogenic turbopumps [160]. Liquid hydrogen, which is typically pumped at a temperature of $\approx$30 K, seems the most likely candidate, but liquid oxygen is also a possibility, if materials with critical temperatures higher than that of YBCO can be used in HTS bearings. The tribological properties of mechanical bearings at cryogenic temperatures are poor, and experience with rocket engines indicates that the bearings of turbopumps are one of the most life-limiting components. In this application, the cryogen is already available and does not impose an extra cost; however the low levitation pressures of present HTS bearings would require a significant redesign of any existing pump. Other applications for HTS bearings in which a cryogenic environment already exists include cryogenic turbine flow metres [161] and cryocoolers for space [29] or terrestrial use. Another application for which a cryogenic environment naturally exists is the use of HTS bearings in a lunar telescope [162]. The drive mechanism of the telescope must be capable of exceedingly fine steps and repeatability, and it must survive and operate in the cold temperatures of the lunar night. Prototype HTS bearings for such a telescope have been constructed and tested [142]. Applications that create a high-value-added product per hour, such as high-speed machine tools or textile spindles, could also justify the added expense of providing a cryogenic environment for HTS bearings [29].

The low magnetic drag of an HTS bearing has suggested its use as a sensitive detector of gas pressure [141]. The possibility of using low-loss superconducting bearings in sensitive gyroscopes has long been recognized [4]. Recently, HTS bearings have been proposed for use in sensitive gravimeters [163]. In this application, subradian oscillations or small angular rotations are observed. If the motion is small enough, the HTS should remain in an elastic regime with all of the flux lines remaining in their pinning centres, and the dissipation should be extremely small.

The hysteretic nature of HTSs has suggested their use in docking vehicles in space [164]. As one vehicle approaches another it would experience a decelerating repulsive force. After the relative velocities have disappeared at a small separation distance, the vehicles would experience an attractive force if their distances tended to separate. Hysteresis is also important in the potential use of HTS as torque couplers and vibration dampers [165]. Apparently, the first successful vacuum tunnelling experiment, which

eventually led to the development of the scanning tunnelling microscope, was made possible by suppression of vibrations with the use of a superconducting bearing [166].

Although this article has focused almost exclusively on rotating HTS bearings, similar physics applies to linear HTS bearings. The stable levitational force suggests application in magnetically levitated conveyor systems in clean-room environments, where high purity requirements mandate no mechanical contact [167, 168]. Linear HTS bearings have also been proposed for microactuators [169].

Acknowledgments

This work was partially supported by the US Department of Energy, Energy Efficiency and Renewable Energy, as part of a programme to develop electric power technology, under contract W-31-109-Eng-38. The author is grateful to T Mulcahy and K Uherka for reviewing an early draft of the manuscript.

References

[1] Arkadiev V 1945 *J. Phys. USSR* **9** 148
[2] Arkadiev V 1947 *Nature* **160** 330
[3] Simon I 1953 *J. Appl. Phys.* **24** 19
[4] Buchhold T A 1960 *Sci. Am.* **202** (3) 74
[5] Schoch K F 1960 *Adv. Cryogen. Eng.* **6** 65
[6] Buchhold T A 1965 *Cryogenics* **5** 216
[7] Condon E U and Maxwell E 1949 *Phys. Rev.* **76** 578
[8] Fritz J J, Gonzalez O D and Johnston H L 1950 *Phys. Rev.* **80** 894
[9] File J, Martin G D, Mills R G and Wakefield K E 1971 *J. Appl. Phys.* **42** 6
[10] Wu M K, Ashburn J R, Torng C J, Hor P H, Meng R L, Gao L, Huang Z J and Chu C W 1987 *Phys. Rev. Lett.* **58** 908
[11] Early E A, Seaman C L, Yang K N and Maple M B 1988 *Am. J. Phys.* **56** 617
[12] Brandt E H 1989 *Science* **243** 349
[13] Brandt E H 1990 *Am. J. Phys.* **58** 43
[14] Moon F C and Hull J R 1990 *Proc. Intersoc. Energy Conv. Eng. Conf.* vol 1, p 425
[15] Hull J R, Mulcahy T M, Lynds L, Weinberger B R, Moon F C and Chang P-Z 1990 *Proc. Intersoc. Energy Conv. Eng. Conf.* vol 3, p 432
[16] Schoenberg D 1936 *Proc. R. Soc.* A **155** 712
[17] Peters P N, Sisk R C, Urban E W, Huang C Y and Wu M K 1988 *Appl. Phys. Lett.* **52** 2066
[18] Adler R J and Anderson W W 1988 *Appl. Phys. Lett.* **53** 2346
[19] Moon F C and Chang P-Z 1990 *Appl. Phys. Lett.* **56** 397
[20] Weeks D E 1990 *Rev. Sci. Instrum.* **61** 195
[21] Weinberger B R, Lynds L and Hull J R 1990 *Supercond. Sci. Technol.* **3** 381
[22] Murakami M 1992 *Melt Processed High-Temperature Superconductors* (Singapore: World Scientific)
[23] Murakami M, Sakai N, Higuchi T and Yoo S I 1996 *Supercond. Sci. Technol.* **9** 1015
[24] Yao X and Shiohara Y 1997 *Supercond. Sci. Technol.* **10** 249
[25] Muraldihar M, Koblishka, M R, Saitoh T and Murakami M 1998 *Supercond. Sci. Technol.* **11** 1349
[26] Kim C-J and Hong G-W 1999 *Supercond. Sci. Technol.* **12** R27
[27] Murakami M (ed) 1998 *Appl. Supercond.* **6** (2-5)
[28] Cardwell D A, Murakami M and Salama K (eds) 1998 *Mater. Sci. Eng.* B **53** (1, 2)
[29] Moon F C 1994 *Superconducting Levitation* (New York: Wiley)
[30] Hull J R and Sheahen T P 1993 *High-Temperature Superconductors* ed T Sheahen (New York: Wiley) p 415
[31] Hull J R 1997 *Spectrum* **34** 20
[32] Hull J R 1998 *Encyclopedia of Electrical and Electronics Engineering* ed J G Webster (New York: Wiley)
[33] Hull J R 2000 *Handbook of Superconducting Materials* ed D Cardwell and D Ginley (Bristol: Institute of Physics) to be published
[34] Moon F C, Weng K-C and Chang P-Z 1989 *J. Appl. Phys.* **66** 5643
[35] Chang P-Z, Moon F C, Hull J R and Mulcahy T M 1990 *J. Appl. Phys.* **67** 4358
[36] Riise A B, Johansen T H and Bratsberg H 1994 *Physica* C **234** 108
[37] Lehndorff B, Kurschner H-G and Lucke B 1995 *Appl. Phys. Lett.* **67** 1932
[38] Hull J R and Cansiz A 1999 *J. Appl. Phys.* **86** 6396
[39] Moon F C, Chang P-Z, Hojaji H, Barkatt A and Thorpe A N 1990 *Japan. J. Appl. Phys.* **29** 1257
[40] Riise A B, Johansen T H, Bratsberg H and Yang Z J 1992 *J. Appl. Phys.* **60** 2294
[41] Murakami M, Gotoh S, Koshizuka N, Tanaka S, Matshushita T, Kambe S and Kitazawa K 1990 *Cryogenics* **30** 390
[42] Schonhuber P and Moon F C 1994 *Appl. Supercond.* **2** 523
[43] Weinstein R, Sawh R, Ren Y and Parks D 1998 *Mater. Sci. Eng.* B **53** 38
[44] Wang J, Yanoviak M M and Raj R 1989 *J. Am. Ceram. Soc.* **72** 846
[45] Johansen T H, Bratsberg H and Yang Z J 1990 *Proc. 2nd World Congress on Superconductors (Houston)*
[46] Unsworth J, Du J, Crosby B J and Macfarlane J C 1993 *IEEE. Trans. Magn.* **29** 108
[47] Shi D, Qu D, Sagar A and Lahiri K 1997 *Appl. Phys. Lett.* **70** 3606
[48] Tent B A, Qu D and Shi D 1998 *Physica* C **309** 89
[49] Tent B A, Qu D, Shi D, Bresser W J, Boolchand P and Cai Z-X 1998 *Phys. Rev.* B **58** 11 761
[50] Yang W M *et al* 1998 *Physica* C **307** 271
[51] Weinberger B R 1994 *Appl. Supercond.* **2** 511
[52] Schonhuber P and Moon F C 1994 *Appl. Supercond.* **2** 523
[53] Lucke B, Kurschner H-G, Lehndorff B, Lenkens M and Piel H 1996 *Physica* C **259** 151
[54] Johansen T H, Riise A B, Bratsberg H and Shen Y Q 1998 *J. Supercond.* **11** 519
[55] Cha Y S, Hull J R, Mulcahy T M and Rossing T D 1991 *J. Appl. Phys.* **70** 6504
[56] Tsuchimoto M, Kojima T, Waki H and Honma T 1994 *Appl. Supercond.* **2** 549
[57] Yang Z J and Hull J R 1996 *J. Appl. Phys.* **79** 3318
[58] Teshima H, Morita M and Hashimoto M 1996 *Physica* C **269** 15
[59] Sagar S, Lahiri, K, Shi D and Yangf Z J 1997 *IEEE Trans. Appl. Supercond.* **7** 1929
[60] Badia A and Freyhardt H C 1998 *J. Appl. Phys.* **83** 2681
[61] Hull J R, Mulcahy T M and Labataille J F 1997 *Appl. Phys. Lett.* **70** 655
[62] Litzkendorf D, Habisreuther T, Wu M, Strasser T, Zeisberger M, Gawalek W, Helbig M and Gornet P 1998 *Mater. Sci. Eng.* B **53** 75
[63] Hull J R 1997 *Adv. Supercond.* **10** 1401
[64] Moon F C 1990 *Appl. Electromagn. Mater.* **1** 29
[65] Sugiura T and Fujimori H 1996 *IEEE Trans. Magn.* **32** 1066
[66] Sugiura T, Matsunaga K, Uematsu Y, Aoyagi T and Yoshizawa M 1997 *Adv. Supercond.* **10** 1349
[67] Basinger S A, Hull J R and Mulcahy T M 1990 *Appl. Phys. Lett.* **57** 2942
[68] Hull J R, Mulcahy T M, Salama K, Selvamanickam V, Weinberger B R and Lynds L 1992 *J. Appl. Phys.* **72** 2089
[69] Johansen T H, Bratsberg H, Yang Z J, Guo S J and Loberg B 1991 *J. Appl. Phys.* **70** 7496

[70] Nemoshkalenko V V, Brandt E H, Kordyuk A A and Nikitin B G 1990 *Physica* C **170** 481
[71] Kordyuk A A and Nomeshkalenko V V 1996 *J. Supercond.* **9** 77
[72] Terentiev A N, Lee H J, Kim C-J and Hong G W 1997 *Physica* C **290** 291
[73] Yang Z J and Hull J R 1997 *IEEE Trans. Appl. Supercond.* **7** 318
[74] Kordyuk A A and Nemosckalenko V V 1997 *IEEE Trans. Appl. Supercond.* **7** 928
[75] Rossman C E, Budnick J I and Weinberger B R 1997 *Appl. Phys. Lett.* **70** 255
[76] Terentiev A N and Harrison J P 1995 *Japan. J. Appl. Phys.* **34** L294
[77] Terentiev A N, Moffat S H, Hughes R A, Preston J S, van Lierop J and Harrison J P 1997 *Cryogenics* **37** 113
[78] Moon F C 1988 *Phys. Lett.* A **132** 249
[79] Hikihara T and Moon F C 1994 *Phys. Lett.* A **191** 279
[80] Hikihara T, Fujinami T and Moon F C 1997 *Phys. Lett.* A **231** 217
[81] Earnshaw S 1842 *Trans. Camb. Phil. Soc.* **7** 98
[82] Braunbek W 1939 *Z. Phys.* **112** 753
[83] Bean C P 1962 *Phys. Rev. Lett.* **8** 250
[84] Bean C P 1964 *Rev. Mod. Phys.* **36** 31
[85] Davis L C, Logothetis E M and Soltis R E 1988 *J. Appl. Phys.* **64** 4212
[86] Davis L C 1990 *J. Appl. Phys.* **67** 2631
[87] Sugiura T, Hashizume H and Miya K 1991 *Int. J. Appl. Electromagn. Mater.* **2** 183
[88] Tsuchimoto M, Kojima T, Takeuchi H and Honma T 1993 *IEEE Trans. Magn.* **29** 3577
[89] Johansen T H, Bratsberg H, Riise A B, Mestl H and Skjeltorp A T 1994 *Appl. Supercond.* **2** 535
[90] Riise A B, Johansen T H and Bratsberg H 1994 *Physica* C **234** 108
[91] Hetland P O, Johansen T H and Bratsberg H 1995 *Appl. Supercond.* **3** 585
[92] Kuze H and Onae A 1995 *J. Appl. Phys.* **77** 770
[93] Sanchez A and Navau C 1996 *Physica* C **268** 46
[94] Hetland P O, Johansen T H and Bratsberg H 1996 *Cryogenics* **36** 41
[95] Hauser A O 1997 *IEEE Trans. Magn.* **33** 1572
[96] Turner L R and Foster M W 1998 *IEEE Trans. Magn.* **34** 3024
[97] Navau C and Sanchez A 1998 *Phys. Rev.* B **58** 963
[98] Yang Z J 1992 *J. Supercond.* **5** 259
[99] Yang Z J 1994 *Appl. Supercond.* **2** 559
[100] Yang Z J and Hull J R 1996 *J. Appl. Phys.* **79** 3318
[101] Fukuyama H and Takizawa 1998 *Proc. Int. Symp. Magn. Bearings (Boston)*
[102] Marinescu M, Marinescu N, Tenbrink J and Krauth H 1989 *IEEE Trans. Magn.* **25** 3233
[103] Braun M, Buszka P, Motylewski T, Przydrozny W and Sliwa C 1990 *Physica* C **171** 537
[104] Kordyuk A A 1998 *J. Appl. Phys.* **83** 610
[105] McMichael C K, Ma K B, Lin M W, Lamb M A, Meng R L, Xue Y Y, Hor P H and Chu W K 1991 *Appl. Phys. Lett.* **59** 2442
[106] Mulcahy T M, Hull J R, Uherka K L, Abboud R G, Wise J H, Carnegie D W, Gabrys C W and Bakis C E 1996 *IEEE Trans. Magn.* **32** 2609
[107] Zannella S, Frangi F and Varesi E 1994 *Nuovo Cimento* D **16** 2061
[108] Marion-Pera M C and Yonnet J P 1994 *IEEE Trans. Magn.* **30** 4743
[109] Tsuchimoto M, Kojima T, Waki H and Honma T 1994 *Appl. Supercond.* **2** 549
[110] Komori M, Matsushita T and Takeo M 1993 *Cryogenics* **33** 1058
[111] Tixador P, Hiebel P, Brunet Y, Chaud X and Gautier-Picard P 1996 *IEEE Trans. Magn.* **32** 2578
[112] Evershed S 1900 *J. Inst. Electr. Eng.* **29** 743
[113] McMichael C K, Ma K B, Lamb M A, Lin M W, Chow L, Meng R L, Hor P H and Chu W K 1992 *Appl. Phys. Lett.* **60** 1893
[114] Chu W K, Ma K B, McMichael C K and Lamb M A 1993 *Appl. Supercond.* **1** 1259
[115] Xia Z, Chen Q Y, Ma K B, McMichael C K, Lamb M, Cooley R S, Fowler P C and Chu W K 1995 *IEEE Trans. Appl. Supercond.* **5** 622
[116] Hennig W, Parks D, Weinstein R and Sawh R-P 1998 *Appl. Phys. Lett.* **72** 3059
[117] Weinstein R, Sawh R, Ren Y and Parks D 1998 *Mater. Sci. Eng.* B **53** 38
[118] Morita M, Nagashima K, Takebayashi S, Murakami M and Sawamura M 1998 *Mater. Sci. Eng.* B **53** 159
[119] Gruss S, Fuchs G, Krabbes, Schatzle P, Fink J, Muller K H and Schultz L 1998 *IEEE Trans. Magn.* **34** 2099
[120] Hull J R, Mulcahy T M, Uherka K L, Erck R A and Abboud R G 1994 *Appl. Supercond.* **2** 449
[121] Hull J R, Mulcahy T M, Uherka K L and Abboud R G 1995 *IEEE Trans. Appl. Supercond.* **5** 626
[122] Mulcahy T M, Hull J R, Uherka K L, Niemann R C, Abboud R G, Juna J and Lockwood J A 1999 *IEEE Trans. Appl. Supercond.* **9** 297
[123] Hull J R, Passmore J L, Mulcahy T M and Rossing T D 1994 *J. Appl. Phys.* **76** 577
[124] Hull J R, Hilton E F, Mulcahy T M, Yang Z J, Lockwood A and Strasik M 1995 *J. Appl. Phys.* **78** 6833
[125] Komori M, Kumamoto M and Kobayashi H 1998 *IEEE Trans. Appl. Supercond.* **8** 79
[126] Nagaya K 1996 *IEEE Trans. Magn.* **32** 445
[127] Kameno H, Miyagawa Y, Takahata R and Ueyama H 1999 *IEEE Trans. Appl. Supercond.* **9** 972
[128] Coombs T A, Campbell A M and Cardwell D A 1995 *IEEE Trans. Appl. Supercond.* **5** 630
[129] Teshima H 1997 *Japan. J. Appl. Phys.* **36** 68
[130] Takamori T, Boland J J and Dove D B 1989 *Appl. Phys. Lett.* **55** 1454
[131] Iwasa Y and Lee H 1997 *Cryogenics* **37** 807
[132] Lee H, Tsuda M and Iwasa Y 1998 *Cryogenics* **38** 419
[133] Tsuda M, Lee H and Iwasa Y 1998 *Cryogenics* **38** 743
[134] Hull J R, Labataille J F, Mulcahy T M and Lockwood J A 1996 *Appl. Supercond.* **4** 1
[135] Weinberger B R, Lynds L, Hull J R and Balachandran U 1991 *Appl. Phys. Lett.* **59** 1132
[136] Teshima H, Tanaka M, Miyamoto K, Nohguchi K and Ninata K 1996 *Physica* C **256** 142
[137] Ehrich F E 1992 *Handbook of Rotor Dynamics* (New York: McGraw-Hill)
[138] Tonoli A and Bornemann H J 1998 *J. Sound Vib.* **212** 649
[139] Martini G, Rivetti A and Pavese F 1990 *Adv. Cryogen. Eng.* **35** 639
[140] Ma K-B, Liu J-R, McMichael C, Bruce R, Mims D and Chu W-K 1991 *J. Appl. Phys.* **70** 3961
[141] Chew A D, Chambers A and Troup A P 1995 *Appl. Supercond.* **3** 327
[142] Lee E, Ma K B, Wilson T L and Chu W K M 1999 *IEEE Trans. Appl. Supercond.* **9** 911
[143] Sugiura T, Tashiro M, Uematsu Y and Yoshizawa M 1997 *IEEE Trans. Appl. Supercond.* **7** 386
[144] Rossman C E and Budnick J I 1998 *Physica* C **295** 304
[145] Terentiev A N 1990 *Physica* C **166** 71
[146] Ternetiev A N and Kuznetsov A A 1990 *Physica* C **169** 112
[147] Terentiev A N and Kuznetsov A A 1992 *Physica* C **195** 41
[148] Krasnyuk N N and Mitrofanov V P 1992 *Superconductivity* **5** 1638
[149] Postrekhin E V, Koscheeva S N and Zhou L W 1995 *Physica* C **248** 311
[150] Hikihara T and Moon F C 1995 *Physica* C **250** 121
[151] Hikihara T, Adachi H, Ohashi S, Hirane Y and Ueda Y 1997 *Physica* C **291** 34
[152] Coombs T A and Campbell A M 1996 *Physica* C **256** 298

[153] Smolyak B M, Babanov M V, Ermakov G V, Smolyak I B and Naumov S V 1998 *Physica* C **302** 23
[154] Smolyak B M, Babanov M V, Ermakov G V, Postrekhin E V, Shou L W, Smolyak I B and Naumov S V 1998 *Mater. Sci. Eng.* B **53** 177
[155] Bornemann H J, Ritter T, Urban C, Zaitsev O, Weber K and Rietschel H 1994 *Appl. Supercond.* **2** 439
[156] Chen Q Y, Xia Z, Ma K B, McMichael C K, Lamb M, Cooley R S, Fowler P C and Chu W K 1994 *Appl. Supercond.* **2** 457
[157] Minami M, Nagaya S, Kawashima H, Sato T and Kurimura T 1997 *Adv. Supercond.* **10** 1305
[158] Miyagawa Y, Kameno H, Takahata R and Ueyama H 1999 *IEEE Trans. Appl. Supercond.* **9** 996
[159] Coombs T A, Campbell A M, Ganney I, Lo W, Twardowski T and Dawson B 1998 *Mater. Sci. Eng.* B **53** 225
[160] Decher R, Peters P N, Sisk R C, Urban E W, Vlasse M and Rao D K 1993 *Appl. Supercond.* **1** 1265
[161] Rivetti A, Martini G, Goria R and Lorefice S 1987 *Cryogenics* **27** 8
[162] Lamb M, Ma K B, Cooley R, Mackey D, Meng R, Chu C W, Chu W K, Chen P C and Wilson T 1995 *IEEE Trans. Appl. Supercond.* **5** 638
[163] Hull J R and Mulcahy T M 1999 *IEEE Trans. Appl. Supercond.* **9** 390
[164] Weinstein R, Parks D Sawh R-P, Obot V, Liu J and Arndt G D 1995 *3rd Int. Symp. on Magnetic Suspension Technology (Tallahassee)*
[165] Ma K B, McMichael C K, Lamb M A and Chu W K 1993 *IEEE Trans. Appl. Supercond.* **3** 388
[166] Binnig G, Rohrer H, Gerber Ch and Weibel E 1982 *Appl. Phys. Lett.* **40** 178
[167] Ogiwara H, Azukizawa T and Morishita M 1993 *Appl. Supercond.* **1** 1185
[168] Minami H and Yuyama J 1995 *Japan. J. Appl. Phys.* **34** 346
[169] Kim Y-K, Katsurai M and Fujita H 1989 *Sensors Actuators* **20** 33